A Mean Field Coarse-Grained Model for Poly(ethylene oxide)-Poly(propylene oxide)-Poly(ethylene oxide) Triblock Copolymer Systems

Fabián A. García Daza,[†] Alexander J. Colville,[‡] and Allan D. Mackie[*,†]

Department d'Enginyeria Química, ETSEQ, Universitat Rovira i Virgili, Avinguda dels Països Catalans 26, 43007 Tarragona, Spain, and Chemical Engineering Department, 313 Snell Engineering Center, Northeastern University, 360 Huntington Avenue, Boston, Massachusetts 02115-5000, United States

E-mail: allan.mackie@urv.cat

Abstract

The microscopic modeling of surfactant systems is of the utmost importance in the understanding of the mechanisms related to the micellization process because it allows for the prediction and comparison with experimental data of diverse equilibrium system properties. In this work we present a coarse-grained model for Pluronics, a trademarked type of triblock copolymers, from simulations based on a Single Chain Mean Field theory (SCMF). This microscopic model is used to quantify the micellization process of

[*]To whom correspondence should be addressed

[†]Department d'Enginyeria Química, ETSEQ, Universitat Rovira i Virgili, Avinguda dels Països Catalans 26, 43007 Tarragona, Spain

[‡]Chemical Engineering Department, 313 Snell Engineering Center, Northeastern University, 360 Huntington Avenue, Boston, Massachusetts 02115-5000, United States

these nonionic surfactants at 37 °C, and has shown to be able to quantitatively reproduce experimental data of the Critical Micelle Concentration (CMC) along with other equilibrium properties. In particular, these results correctly capture the experimental behavior with respect to the lengths of the hydrophobic and hydrophilic moieties of the surfactants for low and medium hydrophobicities. However, for the more highly hydrophobic systems with low CMCs, a deviation is found which has been previously attributed to non-equilibrium effects in the experimental data [García Daza, F. A.; Mackie, A. D. *J. Phys. Chem. Lett.* **2014**, 5, 2027-2032].

Introduction

Poly(ethylene oxide)-Poly(propylene oxide)-Poly(ethylene oxide) molecules, a type of linear triblock nonionic copolymer surfactants commercially available as Pluronics, Synperonics, and Poloxamers, have gained popularity for a wide variety of applications including biomedical uses. Pluronics contain a central hydrophobic poly(propylene oxide) (PPO) chain connected to two hydrophilic poly(ethylene oxide) (PEO) chains. At sufficiently high concentrations of surfactant, the molecules spontaneously self-assemble into micelles[1] and later into worm-like aggregates.[2] The broad use of Pluronics stems from their unique properties in solution as well as their customizable length and size. As a result, it is very valuable to be able to accurately predict the structure, dynamics, and properties of Pluronics under a variety of conditions such as in vivo, and this study works towards that goal.

These nonionic surfactants have been used in a wide variety of important industrial sectors including pharmaceuticals, cosmetics, oil recovery and as drug and gene nanocarriers for targeted drug delivery.[3] Some of the surfactants have been coated on the surface of nanoparticles to improve desirable qualities of the particles such as solubility, stability, and targeting.[4] Recently, medical research has shown some of the copolymers to elicit biological responses in vitro and in vivo.[5] Certain classifications of Pluronics have enhanced gene tran-

scription,[6] improved drug potency of chemotherapeutics such as doxorubicin against cancer cells,[7] and modified other biological responses. The copolymers can be blended into polymeric matrices to form hydrogels and other drug carriers with highly specific release rates.

The self-assembly of micelles is caused by the forces of chemical equilibrium,[1] where the interactions between the hydrophilic and hydrophobic groups with the solvent and each other must all balance with any effects of entropy changes due to organization, therefore, the self-assembly of surfactants into micelles is controlled by changes in free energy. Such assembly into aggregates comes about over a small range of surfactant concentrations. This narrow range can be quantified as a useful parameter known as the Critical Micelle Concentration (CMC),[8,9] which represents the point of spontaneous micelle aggregation from free surfactants. This transformation in conformation and aggregation exhibits changes in the physical and chemical properties of a solution such as surface tension, osmotic pressure, solubilization, detergent activity, turbidity, and conductivity.[10] The transition at the CMC is very important for applications of the product micelles as well as for models of the micellization process.

The CMC of many surfactants has been determined experimentally through a number of techniques including surface tension, light scattering, spectrophotometry, nuclear magnetic resonance, fluorimetry, and capillary electrophoresis.[11] The micellization and subsequent experimental CMC values for Pluronic surfactants has been studied extensively, however, experimental concentrations for PEO-PPO-PEO block copolymer micelles have faced issues in reproducibility and speed.[12] Such inconsistencies and costs have pushed researchers to seek alternative methods of studying micellization.

Computer simulations have been used to predict thermodynamic properties of only a select group of simple surfactants. Thermodynamic parameters of the micellization process for

surfactants include the CMC, phase behavior, and associated free-energy change. Previous works have included the analysis of free energy contributions,[13] molecular dynamics (MD),[14] Monte Carlo simulations (MC)[9] and mean-field models.[15]

MD and MC simulation methods have proven to be effective for the simulation of atom based models of surfactants in the micellization process when the micelles are pre-assembled, however, these methods are computationally expensive for the determination of the CMC and other equilibrium properties when the systems are required to self-assemble[16] due to the slow kinetics of micelle formation. This is particularly the case for Pluronic micelles because of the large size of the surfactants.[17,18] As a result, MD and MC methods have been found to take prohibitive amounts of time to reach equilibrium even for short nonionic diblock surfactants.[14] These computational problems associated with MD and MC simulation efforts suggest that alternative techniques need to be explored in order to be able to adequately study the formation of micelles in surfactant solutions. One such technique is the Single Chain Mean Field theory[19] (SCMF) used in this work where a similar coarse-grained model as in conventional molecular simulations is used, however, the estimation of the equilibrium properties is simplified by solving for single chains in a mean-field of the other species in the system. **In this sense the SCMF is similar to the standard Self-Consistent Field theory[2,18,20] (SCF) where surfactants are modeled as Gaussian chains interacting with surrounding concentration fields. Nonetheless, the possibility of overlapping chains in the SCF comes from its Markovian nature implying the absence of excluded-volume repulsions and as a consequence an incomplete estimation of the free energy of the system. In contrast, the SCMF considers non-Markovian connections between segments of the same chain and thus only non-overlapping configurations are used to estimate the free energy contributions.** The SCMF has already been successfully employed in the study of diblock surfactants[9,15] as well as gemini surfactants[21]and has been recommended specifically for the study of Pluronic micelles.[22] To our knowledge, a comprehensive list of theoretical CMCs for Pluronic micelles has not been

published and the extension of the SCMF to Pluronics in this study attempts to reach this goal.

In the current study, we have conducted a series of simulations within the SCMF to construct a coarse-grained model for the PEO-PPO-PEO surfactants in water for a temperature of 37 °C focused mainly on the reproduction of experimental CMCs. First, the details of the microscopic model and the simulation protocols are given. Afterwards, the related model parameters are optimized and a series of SCMF simulations are implemented for a set of Pluronics to obtain predictions of the CMCs together with the corresponding aggregation numbers and micellar profiles. In the Results and Discussion section the SCMF predictions are compared with the available experimental data including CMCs, aggregation numbers, and the volume fraction profiles. The results are discussed in the context of observed experimental discrepancies manifested by several authors and the deviation found in this work of the CMC between experimental and predicted data for the most hydrophobic surfactants.

Model and Simulation Method

Single Chain Mean Field Theory

In the SCMF scheme the intermolecular energetic contributions of surfactants belonging to an aggregate of size N are taken into account through the interactions of a single coarse-grained chain, representing the surfactant, with a set of concentration fields of solvent and surfactants while the intramolecular interactions are obtained in an exact manner. **The expression for the energy in this system is given in terms of averaged energetic values of configurations of the surfactant, $\{\gamma\}$, weighted by its individual probabilities, $P[\gamma]$, and is given by**

$$\langle E \rangle = N \int d\gamma \, P[\gamma] \Big(U_{intra}[\gamma] + U_{inter}[\gamma] \Big), \tag{1}$$

where $U_{intra}[\gamma]$ is the exact internal energy of conformation γ, and, $U_{inter}[\gamma]$ refers to the intermolecular energy related to **the interactions of the configuration with the other surfactants** and solvent medium and is given as

$$U_{inter}[\gamma] = \frac{N-1}{2} \int d\vec{r}\, d\beta\, P[\beta] U_{inter}[\gamma, \beta, \vec{r}] + \int d\vec{r}\, c_s(\vec{r}) U_{inter}[\gamma, \vec{r}]. \tag{2}$$

The first term on the right side represents the intermolecular surfactant interactions of the conformation γ with the remaining $N-1$ surfactants in the system by means of the interaction with configuration β together with its associated probability $P[\beta]$ and the corresponding energetic contribution $U_{inter}[\gamma, \beta, \vec{r}] = \sum_{i,j} \epsilon_{i,j} \Phi_i(\gamma, \vec{r}) c_j(\beta, \vec{r})$. The terms in this summation are the interaction parameters, $\epsilon_{i,j}$, **together with the interaction volume** $d\vec{r}\, \Phi_i(\gamma, \vec{r})$ **available for configuration** γ **to interact at** $\vec{r}$ **with the remaining conformations** $\{\beta\}$ **through their corresponding concentration,** $c_j(\beta, \vec{r})$**, for the appropriate species** i, j **that make up the surfactant in the coarse grained model.** The second term represents the interaction of configuration γ with the solvent medium through its concentration field $c_s(\vec{r})$ at $\vec{r}$ by means of $U_{inter}[\gamma, \vec{r}] = \sum_i \epsilon_{i,s} \Phi_i(\gamma, \vec{r})$ with respect to the coarse-grained solvent and surfactant-solvent interaction parameters $\epsilon_{i,s}$. The terms given in eq 2 account only for attractive intermolecular interactions, for which the repulsive terms are included by means of steric hard-core repulsions given by the following volume-filling constraint,

$$\phi_s(\vec{r}) + N \sum_i \langle \phi_i^{exc}(\vec{r}) \rangle = 1, \tag{3}$$

which means that all regions of physical space are occupied either by solvent or surfactant molecules by means of the corresponding volume fractions $\phi_s(\vec{r})$ and $\langle \phi_i^{exc}(\vec{r}) \rangle$ respectively, this last term representing the correct excluded-volume contributions. The term inside the angular brackets in eq 3 comes from the single-chain values of $\phi_i^{exc}(\gamma, \vec{r})$, **interpreted as the total physical volume fraction of species** i **of conformation** γ **at** $\vec{r}$ **that cannot be accessed by solvent or other surfactant molecules,** weighted by the individual

probabilities giving as result the average excluded-volume fraction of the surfactant

$$\langle \phi_i^{exc}(\vec{r}) \rangle = \int d\gamma \; P[\gamma] \phi_i^{exc}(\gamma, \vec{r}), \tag{4}$$

and similarly, the concentration fields of the surfactant monomers can be predicted in general from

$$\langle c_i(\vec{r}) \rangle = \int d\gamma \; P[\gamma] c_i(\gamma, \vec{r}). \tag{5}$$

From here, the determination of the associated probabilities $P[\gamma]$ is given by a minimization of the system free energy $\langle F \rangle = \langle E \rangle - T\langle S \rangle$, where the entropy contains the configurational surfactant contributions and the solvent translational entropy

$$\langle S \rangle = -Nk \int d\gamma \; P[\gamma] \log P[\gamma] - k \int d\vec{r} \, c_s(\vec{r}) \log \phi_s(\vec{r}), \tag{6}$$

with k and T as Boltzmann's constant and temperature of the system respectively. Minimizing now $\langle F \rangle$ from $\delta\langle F \rangle / \delta P[\gamma] = 0$ subject to the volume-filling constraint in eq 3 with the inclusion of the Lagrange multipliers $\lambda(\vec{r})$, which in turn can be found from the evaluation of $\delta\langle F \rangle / \delta c_s(\vec{r}) = 0$, provides the individual probabilities in equilibrium

$$P[\gamma] = \frac{e^{-H_N[\gamma]/kT}}{Q}. \tag{7}$$

where Q is the partition function of the system ensuring the normalization of the associated probabilities. Finally, from eq 7 we can establish the SCMF Hamiltonian $H_N[\gamma]$ associated with conformation γ that contains the intramolecular and intermolecular interactions for the corresponding surfactant with the surrounding fields. In addition, intermolecular steric repulsions are also derived from the Lagrange multipliers definition with constraints in eq 3.

The analytical expression of the Hamiltonian is found to be

$$H_N[\gamma] \approx U_{intra}[\gamma] + (N-1)\int d\vec{r}\sum_{i,j}\epsilon_{i,j}\Phi_i(\gamma,\vec{r})\langle c_j(\vec{r})\rangle + \int d\vec{r}\sum_i \epsilon_{i,s}\Phi_i(\gamma,\vec{r})\, c_s(\vec{r}) - kT\int d\vec{r}\,\frac{\log\phi_s(\vec{r})}{v_s}\sum_i \phi_i^{exc}(\gamma,\vec{r}), \quad (8)$$

with v_s as the volume of the solvent molecules. From the set of non-linear equations given in equations 3-5, 7 and 8 it is possible to determine the individual probabilities $P[\gamma]$ in eq 7 and hence the equilibrium properties for aggregates of size N and densities and concentrations through equation 5. In the SCMF approach the necessary inputs are the set of conformations $\{\gamma\}$ of a single surfactant in the simulation box with the estimation of the concentrations $c_i(\gamma,\vec{r})$, excluded-volume fractions $\phi_i^{exc}(\gamma,\vec{r})$ and interaction volume fractions $\Phi_i(\gamma,\vec{r})$ for each conformation.

In order to relate the SCMF to the full micellization process, it is necessary to link the properties of the single micelles to the macroscopic system. This is achieved by calculating the standard chemical potentials of free chains, μ_1^0, and those from micelles of size N, μ_N^0, and substituting them in the well-known equilibrium condition between free surfactants in solution and micelles of an arbitrary size, namely[1]

$$\frac{X_N}{N} = \left(X_1 e^{-(\mu_N^0-\mu_1^0)/kT}\right)^N, \quad (9)$$

where X_N and X_1 are the concentration of aggregated and free surfactants respectively. The calculation of the standard chemical potential in the SCMF can be achieved in terms of the following expression[23] which has been used in earlier studies related with the prediction of equilibrium properties for surfactants systems in solvent medium such as poly(ethylene

oxide) alkyl ethers[15] and more recently a series of nonionic Gemini surfactants,[21]

$$\frac{\mu_N^0 - \mu_1^0}{kT} \approx -\log\left(\frac{V}{N}\frac{\sum_\gamma e^{-H_N[\gamma]/kT}/W[\gamma]}{\sum_\gamma e^{-H_1[\gamma]/kT}/W[\gamma]}\right), \tag{10}$$

where $H_1[\gamma]$ is the Hamiltonian for surfactants in the bulk solution, V is the volume of the simulation box and $W[\gamma]$ is the statistical weight associated with the Rosenbluth and Rosenbluth algorithm to generate non-overlapping chain conformations.[24]

Simulation Protocols

In this work the Pluronic block copolymers are modeled as linear chains composed of two kinds of beads with the same diameter σ; the first one representing the hydrophilic CH_2CH_2O groups and the second the hydrophobic $CH(CH_3)CH_2O$ groups, **the choice of the same size of the EO and PO units is similar to that employed by other research groups for coarse-grained models of Pluronic surfactants.[25,26]** The distance between the centers of two consecutive beads is taken to be σ. The chain stiffness, as indicated by the number of Kuhn segments, has been included by using rigid sections of four consecutive monomers in the case of PO and five monomers in the case of EO species[27,28] **whilst the joints between the segments are free to rotate**, see for instance Figure 1. **The intermolecular interactions in eq 8 are modeled by means of square well potentials with a hard core repulsive interaction up to σ and then an attractive well up to r_{int}. The interaction radius r_{int} has been adjusted to a value of 1.62σ for all species composing the surfactant in order to have a coordination number of 26 as was used in previous models.[15,21] This gives a volume for attractive interactions of $v_{int} = 4/3\pi(r_{int}^3 - \sigma^3)$ for each monomer.** Three independent intermolecular interactions have been used, namely, EO-Solvent, PO-Solvent and EO-PO with their corresponding numerical values $\epsilon_{EO,S}$, $\epsilon_{PO,S}$ and $\epsilon_{EO,PO}$. With these assumptions for the interactions and species, we can state the specific complete non-linear set of equations in order to describe

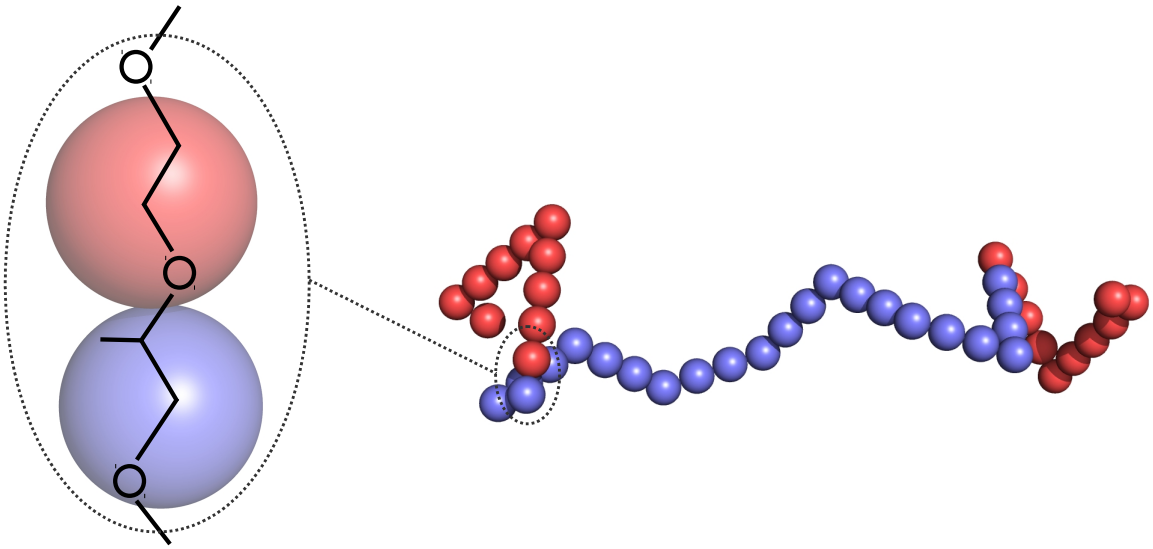

Figure 1: Coarse-grained model for Pluronic L44 $EO_{10}PO_{23}EO_{10}$. Right: Typical self-avoiding conformation generated by the Rosenbluth and Rosenbluth method. Left: Detailed coarse-grained extrapolation in the SCMF technique employed in this work, red and blue beads represents EO and PO groups respectively

the equilibrium properties. In the first place, the indexes in the whole equations system are reduced to $i,\ j = EO, PO$, besides, in the Hamiltonian in eq 8 we have to relate the interaction parameter $\epsilon_{i,j}$ with the analogous Flory-Huggins parameter in the symmetric case $\chi_{ij} = \chi_{ji}$ by means of $\epsilon_{i,j} = kT\chi_{ij}/z$, where $z = 26$ is the coordination number, this choice will affect the excluded-volume term in the SCMF Hamiltonian, for more details see Ref. 15. The Hamiltonian can be written now as

$$\begin{aligned} H_N[\gamma] \approx\ & U_{intra}[\gamma] + (N-1)\frac{kT}{z}\int d\vec{r}\sum_{i\neq j}\chi_{ij}\Phi_i(\gamma,\vec{r})\langle c_j(\vec{r})\rangle + \frac{kT}{z}\int d\vec{r}\sum_i \chi_{is}\,\Phi_i(\gamma,\vec{r})\,c_s(\vec{r}) \\ & -kT\int d\vec{r}\,\frac{\log\phi_s(\vec{r})}{v_s}\sum_i \phi_i^{exc}(\gamma,\vec{r}). \end{aligned} \tag{11}$$

Once the relevant intermolecular interactions and the species describing the surfactant and solvent in the coarse-grained are defined, the SCMF equations can be solved. To do so, we divide the procedure into two stages. In the first stage, **a set of non-overlapping conformations $\{\gamma\}$ are randomly generated according to the Rosenbluth and Rosenbluth algorithm[24]** in a simulation box of volume V, and, all the intrinsic proper-

ties such as concentrations $c_i(\gamma, \vec{r})$, excluded-volume fractions $\phi_i^{exc}(\gamma, \vec{r})$, interaction volume fractions $\Phi_i(\gamma, \vec{r})$ and intramolecular energy $U_{intra}[\gamma]$ are calculated for every conformation γ. In the second, the SCMF system of equations are solved self-consistently, that is, from the calculated fields $\langle c_i(\vec{r})\rangle$ and $\langle \phi_i^{exc}(\vec{r})\rangle$ in equations 4 and 5 a calculation of $\phi_s(\vec{r})$, $H_N[\gamma]$ and the corresponding probability $P[\gamma]$ can be realized by means of equations 3, 7 and 11 respectively, enabling again the calculation of the mean fields over the calculated probabilities making the whole process self-consistent. Once the structural characteristics are assigned, only the intermolecular interaction parameters $\chi_{EO,S}$, $\chi_{PO,S}$ and $\chi_{EO,PO}$, need to be determined. For this purpose, we have performed an error minimization of the difference between predicted and experimental CMCs by means of the gradient method. To capture the overall CMC dependence with respect to the numbers of EO and PO monomers we have chosen to optimize the experimental CMCs for three Pluronics surfactants; two in which the number of EO units are lower than the corresponding PO units L44 and L64, and F87, a surfactant which has significantly more EO than PO units.

Optimization Procedure

To find the optimal values of the Flory-Huggins parameters we take **as initial estimates,** $\chi_{EO,S} = 0.4$ **and** $\chi_{PO,S} = 2.0$ **from Ref. 29, and** $\chi_{EO,PO} = 0.006$ **from references 30 and 31. These parameters are obtained directly or indirectly by fitting to experimental data.** To continue, we start by considering the minimization of the function

$$F[\chi] = \frac{1}{n}\sum_{i=1}^{n}\frac{\left(CMC_i^{sim} - CMC_i^{exp}\right)^2}{s_i^2}, \tag{12}$$

where $n = 3$ is the total number of data which in our case are the experimental CMCs for Pluronics L44, L64 and F87 represented by CMC_i^{exp} with its associated uncertainty s_i^2 and the SCMF predictions CMC_i^{sim}. The minimization procedure can be done via the gradient

method[32] by determining in an iterative scheme the optimal values from

$$\chi_j^{new} = \chi_j^{old} - \alpha \nabla_j F[\chi^{old}], \tag{13}$$

where α is the step size and the index j refers to the energy parameter to be adjusted. In particular from eq 12 we can state

$$\nabla_j F[\chi] = \frac{2}{3} \sum_{i=1}^{3} \frac{(CMC_i^{sim} - CMC_i^{exp})}{s_i^2} \frac{\partial CMC_i^{sim}}{\partial \chi_j}. \tag{14}$$

To find the derivatives in the last equation we can start from the definition of CMC^{sim} adopted in this work, namely, that the CMC is taken based on the micelle of size M with minimum standard chemical potential, $\log CMC_i^{sim} = \min\left(\frac{\mu_N^0 - \mu_1^0}{kT}\right) = \left(\frac{\mu_M^0 - \mu_1^0}{kT}\right)$. The relevant derivatives for this specific case are then $\partial CMC_i^{sim}/\partial \chi_j = CMC_i^{sim}\,(\partial/\partial\chi_j)\,[(\mu_M^0 - \mu_1^0)/kT]$. To develop the partial derivative we made use of the relation between the standard chemical potentials in the SCMF theory given in eq 10

$$\frac{\partial CMC_i^{sim}}{\partial \chi_j} \approx -\frac{CMC_i^{sim}}{kT}\left[\frac{\sum_\gamma e^{-H_1[\gamma]/kT}/W[\gamma]}{Q_1}\frac{\partial H_1[\gamma]}{\partial \chi_j} - \frac{\sum_\gamma e^{-H_M[\gamma]/kT}/W[\gamma]}{Q_M}\frac{\partial H_M[\gamma]}{\partial \chi_j}\right], \tag{15}$$

where $Q_1 = \sum_\gamma e^{-H_1[\gamma]/kT}/W[\gamma]$ and $Q_M = \sum_\gamma e^{-H_M[\gamma]/kT}/W[\gamma]$ are the unbiased partition functions for free and aggregated chains respectively. From the SCMF Hamiltonian in eq 11, and assuming that, the concentration fields and the probabilities remain invariant with respect to the interaction parameters close to the minimum of $F[\chi]$, we can find in general the following set of partial derivatives

$$\begin{aligned}
\frac{\partial H_N[\gamma]}{\partial \chi_{EO,PO}} &\approx \frac{\partial U_{intra}[\gamma]}{\partial \chi_{EO,PO}} + (N-1)\frac{kT}{z}\int d\vec{r}\,\left[\Phi_{EO}(\gamma,\vec{r})\langle c_{PO}(\vec{r})\rangle + \Phi_{PO}(\gamma,\vec{r})\langle c_{EO}(\vec{r})\rangle\right], \\
\frac{\partial H_N[\gamma]}{\partial \chi_{EO,S}} &\approx \frac{kT}{z}\int d\vec{r}\,\Phi_{EO}(\gamma,\vec{r})\,c_s(\vec{r}), \\
\frac{\partial H_N[\gamma]}{\partial \chi_{PO,S}} &\approx \frac{kT}{z}\int d\vec{r}\,\Phi_{PO}(\gamma,\vec{r})\,c_s(\vec{r}).
\end{aligned} \tag{16}$$

This set of equations can be exactly determined in the SCMF simulations for every surfactant chosen to adjust the energy parameters. With this, the fitting procedure for the energy parameters can be done by means of eq 13. To this end, the partial derivatives in eq 14 must be solved through the values given in eq 15 which in turn can be evaluated from the SCMF results obtained in order to calculate the expressions in equations 16.

The coarse-grained dimensions as well as the optimized energy interaction values are presented in Table 1 upon completion of the fitting process. As can be seen, the final values are close to the parameters derived from experiment thus validating the physical model that we have used in our study. Although the differences from the initial guesses are small, they do have a significant effect on the CMC values, and the optimization procedure gives an important improvement in the final fit. The success of the optimization can be observed by a decrease of the objective function in eq 12 from 47.2 to 2.7 when going from the initial guesses, $\chi_{PO,S} = 2.001$, $\chi_{EO,S} = 0.48$, $\chi_{EO,PO} = 0.006$ **(these values were used after a preliminary study rather than the aforementioned literature Flory-Huggins parameters), to the fitted values of** $\{\chi_{i,j}\}$ **respectively, indicating that the difference between the experimental and SCMF results is close to the reported experimental error.** For the optimization procedure and final results a series

Table 1: Coarse-grained structural and energetic specifications

Diameter (σ)	1.0
Bond length (σ)	1.0
Interaction radius (σ)	1.62
EO-PO interaction parameter ($\chi_{EO,PO}$)	0.006
EO-S interaction parameter ($\chi_{EO,S}$)	0.5
PO-S interaction parameter ($\chi_{PO,S}$)	2.1

of simulations were performed where space was discretized into concentric layers separated by a distance $\delta = 0.8\sigma$ for shorter surfactants with less than 100 monomers, while for longer surfactants we assume $\delta = 1.4\sigma$. In all simulations the radius of the first layer is taken

to be 2δ to improve statistics. This choice provides a one-dimensional spherical symmetry where the only coordinate is the radial distance to the center of the simulation box and is supported by experimental evidence using Small Angle Neutron Scattering (SANS),[33] Static Light Scattering (SLS) as well Dynamic Light Scattering (DLS)[34] which suggest a spherical shape for micellar aggregates of Pluronic systems for concentrations close to and above the CMC. Depending on the Pluronic under study, we used simulation boxes with dimensions between $40 \times 40 \times 40$ and $100 \times 100 \times 100$ in units of the beads diameters σ. Between 5 to 10 million of conformations $\{\gamma\}$ were generated for each Pluronic, the simulations were run on 12-core Intel machines, 24-core and 32-core AMD machines with a RAM memory of 60Gb, 30Gb and 120Gb respectively.

Results and Discussion

In Table 2 the physical properties of the Pluronics $EO_nPO_mEO_n$ at a temperature of 37°C are given including: the molecular weight MW, the number of PO and EO units (m and 2n respectively), the predicted CMCs and aggregation number values of the SCMF from this work together with available experimental data. The CMCs reported in this work follow the expected behavior with respect to the length of the hydrophobic PO units. An increase of the PO length increases the repulsive interaction between the surfactant and solvent medium causing a decrease in free energy of micellization thus yielding a lower CMC, together with an increase in the aggregation number. The increase in aggregation number occurs as additional PO monomers increases the available volume to be occupied by the hydrophobic species that can be accommodated in the core of the micelle. Both of these results are exemplified for the cases of Pluronics F68, F88, and F127 where the hydrophilic contribution is almost constant, see Table 2. In the reverse case, an increase of the EO units while the number of PO units remains constant was shown to raise the solubility of the Pluronics in the solvent medium leading to a gradual increase in the CMC. The increase in the number of EO units leads to higher repulsive interactions between hydrophilic units in the corona

Table 2: Physical properties and predictions for Pluronics block copolymers under study

				Aggregation Number		CMC [mol/L]	
Polymer	MW	m	2n	Pred.	Exp.	Pred.	Exp.[a]
L44	2200	23	20	145(1)	-	$4.00(0.01)\times10^{-3}$	3.6×10^{-3}
L64	2900	30	26	187(7)	37[b]	$3.55(0.04)\times10^{-4}$	4.8×10^{-4}
P65	3400	29	36	145(12)	11-21[c]	$0.84(0.01)\times10^{-3}$	2.94×10^{-3}[j]
F68	8400	29	152	33(1)	22[d]	$18.9(0.5)\times10^{-3}$	0.48×10^{-3}, $>8.33\times10^{-3}$[k]
P84	4200	43	34	279(10)	44-54[e]	$3.87(0.05)\times10^{-6}$	71×10^{-6}
P85	4600	40	52	218(4)	57(16)[f]	$2.55(0.03)\times10^{-5}$	6.5×10^{-5}
F87	7700	40	122	66(10)	-	$1.77(0.04)\times10^{-4}$	0.91×10^{-4}
F88	11400	39	208	46(11)	17[g]	$6(1)\times10^{-4}$	2.5×10^{-4}
F98	13000	45	236	40(9)	-	$1.51(0.05)\times10^{-4}$	0.77×10^{-4}
P105	6500	56	74	318(17)	-	$1.54(0.05)\times10^{-7}$	62×10^{-7}[l]
F127	12600	65	200	120(16)	145[h]	$1.3(0.3)\times10^{-7}$	28.0×10^{-7}
F108	14600	50	266	34(10)	13(3)[i]	$2.0(0.3)\times10^{-5}$	2.2×10^{-5}

[a] Taken from Ref. 35 measured through pyrene solubilization technique at 37 °C, unless otherwise specified; [b] From Ref. 36 at 37.5 °C using SANS; [c] In the range of 36-40 °C from Ref. 37 obtained from SLS; [d] At 54 °C from reference 21 cited in Ref. 38; [e] Based on SANS in a range 35-40 °C from Ref. 39; [f] From Light scattering and centrifugation at 37 °C from Ref. 38; [g] At 40 °C from Ref. 40; [h] From Ref. 28 at 35 ° based on SANS; [i] At 37 °C from Ref. 38; [j] Using dye solubilization technique at 36 °C from Ref. 41; [k] Taken from Ref. 41 at 40 °C; [l] Taken from Ref. 42 at 37 °C;

of the micelle forcing the formation of micelles with smaller aggregation numbers. These expected trends were evidenced within all three of the subdivisions of Table 2.

From an analysis of the aggregation numbers presented in Table 2 clear differences can be observed between the experimental and SCMF values. In some cases the experimental data reported by different groups are similar, for instance for P85 where Mortensen and Pedersen [33] using SANS reported aggregation numbers 37-78 in a range 20-40 °C similar to the value 57(16) given by Kabanov et al. [38] at 37°C and the values 37-55 based on SANS with a concentration of 1-5% at 40 °C reported by Goldmints et al.. [43] However, in other cases the aggregation numbers derived from experimental measurements can be highly variable, for example, Yang et al. [36] reported a value of 37 for a temperature of 37.5 °C in the case of L64, however, Wu et al. [44] using SANS reported an aggregation number of 69(7) at 35 °C, in contrast to Almgren et al. [45] who reported a value of 19 for 40 °C. These values are contrary to the expected increase in aggregation number with an increase of temperature. A similar situation is presented in the case of copolymer F127 where Wanka et al. [37] and Mortensen [28] presented aggregation numbers of 82 and 145 respectively for a temperature of 35 °C. In the case of F108 where Alexandridis et al. [8] reported aggregation numbers of 43-61 between 35 and 40 °C in contrast to the value of 13 for a temperature 37°C reported by Kabanov et al. [38] giving a difference of over three times. These contrasts between reported values may be due to the type of experiment and the model considered to describe the physical properties of the micelles, such as in the case of results given by DLS and SLS and discussed by Nolan et al. [34] and Yang et al.. [36] **Despite these differences between experimental values, the SCMF predictions are in general much larger. This difference may be due to the model being too simple to correctly capture the correct fine balance between entropic and enthalpic factors. It may also be due to the approximations used in the SCMF itself. For example, in this work a spherical symmetry is assumed for the micelles without fluctuations, which may affect the micelle free energy of formation by small fractions of kT. Although small compared to the formation of the micelle, these approximations may affect the preferred aggregation number.[9,15] Despite this, the model is able to correctly reproduce the qualitative trends such as a**

decrease of the aggregation number with an increase of the EO units while maintaining the PO units relatively constant as in the case of P84, P85, F87, F88, which has also been observed experimentally for P104, F108 by Alexandridis et al.,[8] P85, F87, F88 by Mortensen and Brown[46] and P103, P104, P105 by Nolan et al..[34] Moreover, an increase in the aggregation number with the number of PO units while EO monomers remains constant is also observed, as in the case of P65, L64 and P84, and has been experimentally reported by Booth and Attwood[47] for a series of Pluronic surfactants.

A comparison between experimental CMC values and those determined with SCMF from Table 2 can be found in Figure 2. In general, a good quantitative agreement between experimental

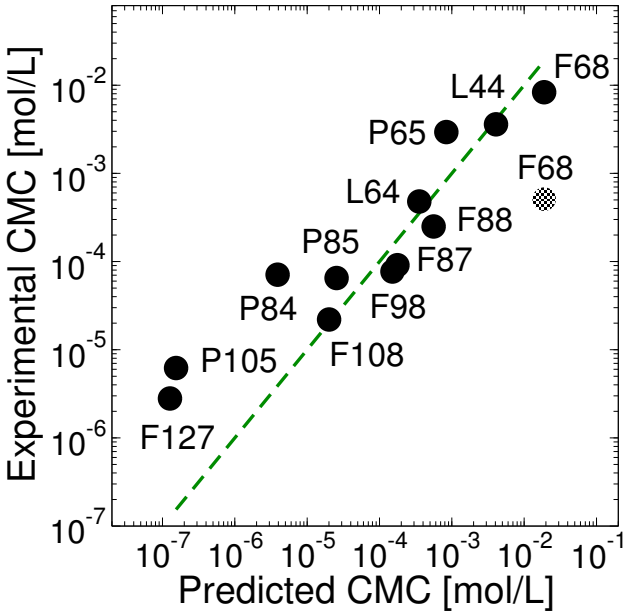

Figure 2: Experimental CMC versus theoretical values predicted in the SCMF scheme for Pluronics studied in this work. Dashed line represents the ideal scenario where experimental and theoretical values match exactly. Error bars in theoretical data are smaller than the diameter of the filled circles

and predicted values can be observed. **For CMCs above 10^{-6} mol/L, most data points are close to the dashed line indicating an excellent quantitative agreement between the SCMF predictions and the experimental values giving a high level of confidence in the model results**. Nevertheless, this is not the case for F68, where two values are given. This is mainly because of the discrepancy between the experimental data reported by Batrakova et al.[35]

and Alexandridis et al..[41] In the latter, the reported CMC above 40 °C is 8.33×10^{-3}mol/L and 11.9×10^{-3} mol/L for 33 °C, this establishes an interval for our target of 37 °C, and supports the idea that in the case of F68 the CMC for a temperature of 37 °C could be near to 10^{-2} mol/L which is in the same order of magnitude as the value reported in this work, although contrary to the value reported by Batrakova et al.[35] which is of the order of 10^{-4} mol/L. This is also supported when comparing the experimental CMCs for a selection of Pluronics in Table 2 with the same PO weight but varying the EO presence; for example, i) in the case of P105 and F108 an increase close to three times in EO content results in an increase of the CMC within the same proportion, ii) similar to P85 and F88, where the hydrophilic units increase four times as well as the corresponding CMCs, hence, an extrapolation to the case of L64 and F68 where the PEO increases five times lead one to expect a similar tendency in the CMC value. Another exception in Figure 2 is that of the most hydrophobic Pluronics P105 and F127 together with P84 which reveal underpredicted values by over one order of magnitude with respect to experimental data.

In order to understand the nature of such discrepancies we have selected a series of Pluronics with hydrophilic units in a specific range which ensures that the changes in the CMC are not significantly affected by the increase or decrease of EO units in this interval. In this case, the effect of the hydrophobic PO length on the CMC can be better appreciated. Specifically, we have considered those Pluronics that contain EO units in the range of 20-74. The CMC dependence when hydrophobic PPO units increases in both experimental and predicted values with the SCMF can be observed in Figure 3. Below 40 PO units there is a good agreement between predictions and experimental values that corresponds to high CMCs, however, above value 43 PO units (Pluronic P84) a strong deviation from the linear behavior in the experimental data is observed and is not predicted in the results of the model implemented in this work.

Following this procedure we can also analyze those surfactants with a total number of hydrophilic units EO in the range 122-266, also including the experimental CMCs reported by Alexandridis et al.[41] in a range of temperature between 35 and 40 °C with the exception of F68 (n=29) whose lowest temperature is 33 °C, the resulting graph is shown in Figure 4.

As can be observed, the experimental values reported in Ref. 41 for CMCs above 10^{-5} mol/L are

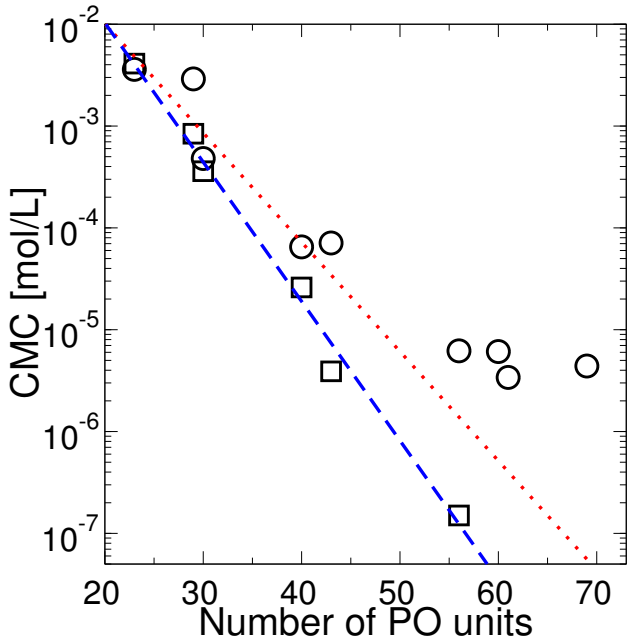

Figure 3: CMC dependence with respect to the hydrophobic length of Pluronics $EO_nPO_mEO_n$ for short head lengths ($20 \leq 2n \leq 74$). Empty circles refer to experimental data given in Table 2 with exception of the three most hydrophobic copolymers (P103, P104 and P123 respectively) which are not included in the table but are given in Ref. 35. Empty squares are SCMF predictions together with the best fit represented by the dashed blue lines, the red dotted line is the best fit for the four highest CMC experimental points

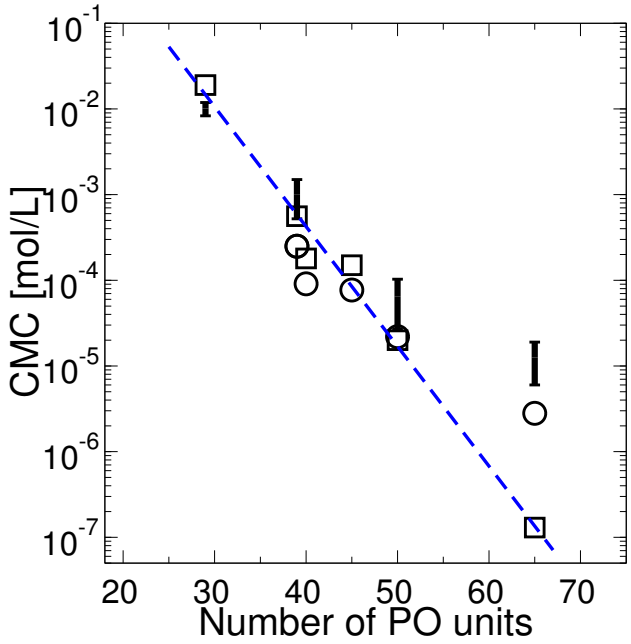

Figure 4: CMC dependence with respect to the hydrophobic length of Pluronics $EO_nPO_mEO_n$ for long head groups ($122 \leq 2n \leq 266$). Empty circles refers to experimental data reported in Ref. 35 which are given in Table 2, bars are the CMCs in a temperature range between 35 and 40 °C given in Ref. 41 while empty squares are the SCMF predictions together with the best fit represented by the dashed blue line

close to the predictions of this work. **However, on increasing the hydrophobic units above 50 PO units, a deviation between experiment and SCMF is found.** This break in the logarithmic CMC behavior with respect to high hydrophobic units is similar to the experimental reports for diblock copolymers[48] and gemini surfactants.[49] From a theoretical point of view, free energy models do not predict such a deviation.[13] Also recent simulations using Grand-Canonical MC simulations for nonionic surfactants exhibit the usual exponential decrease rejecting the collapse of the hydrophobic block as an explanation for such a deviation.[50] Indeed, our previous work for Gemini surfactants suggests that this deviation is because the experimental results are not true equilibrium values due to the large time scales found for these systems.[21] These non-equilibrium effects would explain the discrepancy between experimental P105 and F127 CMCs in comparison to the values reported in this work. **In the case of P84 the CMC values are higher and are not expected to be affected by equilibration issues. However, the experimental data for the CMC of P84 is clearly inconsistent with that of P85; where despite having a larger number of PO and lower EO units, which is expected to give a lower CMC, P84 has**

a larger CMC. This suggests that the discrepancy between experimental and SCMF values for P84 may come from experimental issues different from non-equilibrium effects.

Although aggregates conformed by real conformations as in the usual MD, MC, or DPD simulations cannot be obtained from the SCMF results, it is possible to construct schematic diagrams of the aggregates for surfactants under study from the set of the configurations with the highest probability $\{P[\gamma]\}$. In particular, a micelle for Pluronic F68 is shown in Figure 5, where the snapshot is generated for visualization purposes and should not be interpreted as a real aggregate. As can be observed, the micelles have

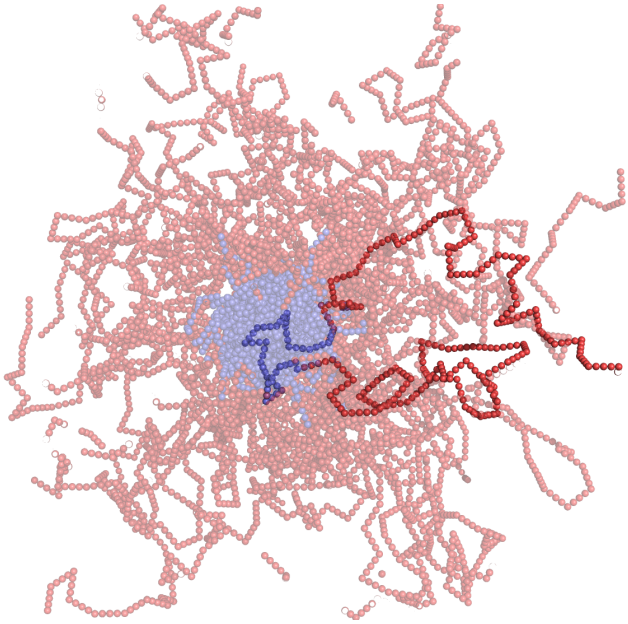

Figure 5: Cross-section **scheme** of an aggregate for Pluronic F108 ($EO_{133}PO_{50}EO_{133}$) for an aggregation number of 34. **The conformation with the highest probability is highlighted while the remaining configurations** are half of the next 33 most probable conformations. Red beads represent the PEO units forming the corona while the PPO units are represented in blue.

a large concentration of hydrophobic PO units in its core which decreases with respect to distance from the center of the micelle. This core is surrounded by a non-uniform shell of hydrophilic EO units that starts to increase from the center of the micelle reaching a maximum value and then decays smoothly with distance. A quantitative description of the density profiles of the micelle is presented in Figure 6.

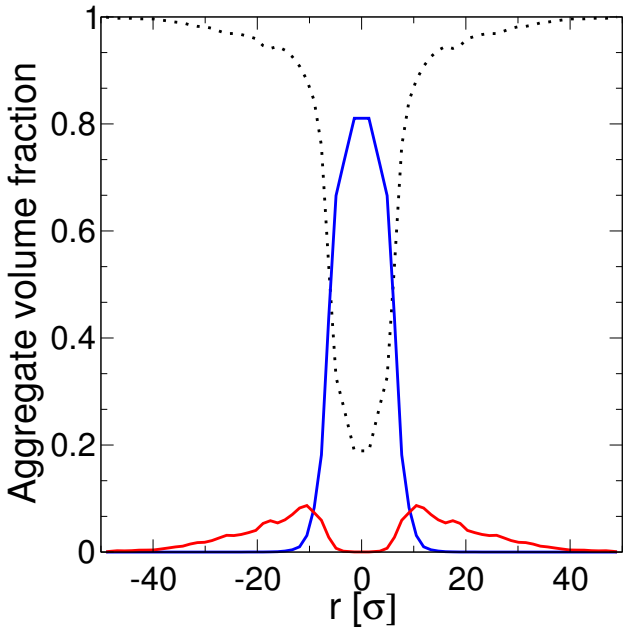

Figure 6: Volume fraction profile for the most stable micelle in the case of Pluronic F108 with an aggregation number $N = 34$. Blue lines represents the PO percentage inside and outside the micelle, while red lines refers to the volume fraction of EO units and black dotted lines are related to the corresponding profile of the solvent

In all cases under study a similar behavior in the equilibrium state volume fraction profile has been observed where the shape of the PO and EO volume fractions depends on their corresponding number of units. The number of PO and EO units of a chosen Pluronic system was shown to modify the solvent profile which is found to be between 20 and 30% at the center of the micelle. This hydration in the center of the micelle has been reported in several simulation works,[2,17,18,20,22] and also derived from the analysis from SANS data for a variety of Pluronics: P85 with a concentration of 5% was found to contain a water content in the core between 60 and 10% for a range of temperature from 31.4 to 40 °C,[43] P84 and P104 at temperatures 35 and 45 °C in concentrations 2.6 and 4.2% respectively[39] contained water content fractions in the core of 20% and 6%, and L64 at a temperature of 37.5 °C and concentration 2.5% was reported to have a fraction of solvent in the core of 40% and 80% in the corona.[36]

Conclusions

We have presented a coarse-grained model for Pluronic systems for 37 degrees Celsius based on SCMF simulations. The estimates of our model for the CMC are found to be in excellent agreement with experimental data for a wide range of surfactants. **On the other hand, the SCMF aggregation numbers are generally much larger than the ones reported from experiments. However, it is difficult to extract the aggregation numbers from the experiments and significant discrepancies between different groups can be found in the literature.** Our findings reveal that an increase of PO units with EO units held relatively constant yields a decrease in the CMC and an increase in the aggregation number. Increasing the hydrophilic EO units results in a slight increase in the CMC and a decrease in the aggregation number. This overall scenario agrees qualitatively with the available experimental and theoretical reports. From a comparison between our CMC predictions and available experimental data, we find evidence of a deviation from the expected exponential trend in the case of experimental CMCs for the most hydrophobic Pluronics. **Based on our confidence of the CMCs predicted in this work when comparing with experimental data down to 10^{-6} mol/L and previous SCMF and MC studies, we suggest that this deviation can be explained as a consequence of non-equilibrium effects in the experiments**.

Acknowledgement

F.A.G.D. acknowledges financial support from URV through his Ph.D. scholarship.

References

(1) Israelachvili, J. N. *Intermolecular and Surface Forces*; Elsevier: San Diego, CA, 2011.

(2) Linse, P. Micellization of Poly(ethylene oxide)-Poly(propylene oxide) Block Copolymers in Aqueous Solution. *Macromolecules* **1993**, *26*, 4437–4449.

(3) Park, T.; Cohen, S.; Langer, R. Controlled drug delivery using polymer/pluronic blends. US Patent 5330768, 1994.

(4) Batrakova, E. V.; Kabanov, A. V. Pluronic block copolymers: Evolution of drug delivery concept from inert nanocarriers to biological response modifiers. *J. Controlled Release* **2008**, *130*, 98–106.

(5) Murhammer, D. W.; Goochee, C. F. Scaleup of Insect Cell Cultures: Protective Effects of Pluronic F-68. *Nat. Biotechnol.* **1988**, *12*, 1411–1418.

(6) Sriadibhatla, S.; Yang, Z.; Gebhart, C.; Alakhov, V. Y.; Kabanov, A. Transcriptional activation of gene expression by pluronic block copolymers in stably and transiently transfected cells. *Mol. Ther.* **2006**, *13*, 804–813.

(7) Alakhova, D. Y.; Zhao, Y.; Li, S.; Kabanov, A. V. Effect of Doxorubicin/Pluronic SP1049C on Tumorigenicity, Aggressiveness, DNA Methylation and Stem Cell Markers in Murine Leukemia. *PLoS One* **2013**, *8*, e72238.

(8) Alexandridis, P.; Nivaggioli, T.; Hatton, T. A. Temperature Effects on Structural Properties of Pluronic P104 and F108 PEO-PPO-PEO Block Copolymer Solutions. *Langmuir* **1995**, *11*, 1468–1476.

(9) Mackie, A. D.; Panagiotopoulos, A. Z.; Szleifer, I. Aggregation Behavior of a Lattice Model for Amphiphiles. *Langmuir* **1997**, *13*, 5022–5031.

(10) Rangel-Yagui, C. O.; Pessoa Jr, A.; Tavares, L. C. Micellar solubilization of drugs. *J. Pharm. Pharm. Sci.* **2005**, *8*, 147–163.

(11) Loh, W. In *Encyclopedia of Surface and Colloid Science, Second Edition*; Somasundaran, P., Ed.; Encyclopedia of Surface and Colloid Science; Taylor & Francis: Boca Raton, FL, 2006; Vol. 2; pp 1014–1025.

(12) Goldmints, I.; Holzwarth, J. F.; Smith, K. A.; Hatton, T. A. Micellar Dynamics in Aqueous Solutions of PEO-PPO-PEO Block Copolymers. *Langmuir* **1997**, *13*, 6130–6134.

(13) Camesano, T. A.; Nagarajan, R. Micelle Formation and CMC of Gemini Surfactants: A Thermodynamic Model. *Colloids Surf. A* **2000**, *167*, 165 – 177.

(14) Levine, B. G.; LeBard, D. N.; DeVane, R.; Shinoda, W.; Kohlmeyer, A.; Klein, M. L. Micellization Studied by GPU-Accelerated Coarse-Grained Molecular Dynamics. *J. Chem. Theory Comput.* **2011**, *7*, 4135–4145.

(15) Gezae Daful, A.; Baulin, V. A.; Bonet Avalos, J.; Mackie, A. D. Accurate Critical Micelle Concentrations from a Microscopic Surfactant Model. *J. Phys. Chem. B* **2011**, *115*, 3434–3443.

(16) Carbone, P.; Avendao, C. Coarse-grained methods for polymeric materials: enthalpy- and entropy-driven models. *Wiley Interdiscip. Rev.: Comput. Mol. Sci.* **2014**, *4*, 62–70.

(17) Bedrov, D.; Smith, G. D.; Yoon, J. Structure and Interactions in Micellar Solutions: Molecular Simulations of Pluronic L64 Aqueous Solutions. *Langmuir* **2007**, *23*, 12032–12041.

(18) de Bruijn, V. G.; van den Broeke, L. J. P.; Leermakers, F. A. M.; Keurentjes, J. T. F. Self-Consistent-Field Analysis of Poly(ethylene oxide)-Poly(propylene oxide)-Poly(ethylene oxide) Surfactants: Micellar Structure, Critical Micellization Concentration, Critical Micellization Temperature, and Cloud Point. *Langmuir* **2002**, *18*, 10467–10474.

(19) Ben-Shaul, A.; Szleifer, I.; Gelbart, W. M. Chain organization and thermodynamics in micelles and bilayers. I. Theory. *J. Chem. Phys.* **1985**, *83*, 3597–3611.

(20) Hurter, P. N.; Scheutjens, J. M. H. M.; Hatton, T. A. Molecular Modeling of Micelle Formation and Solubilization in Block Copolymer Micelles. 1. A Self-Consistent Mean-Field Lattice Theory. *Macromolecules* **1993**, *26*, 5592–5601.

(21) García Daza, F. A.; Mackie, A. D. Low Critical Micelle Concentration Discrepancy between Theory and Experiment. *J. Phys. Chem. Lett.* **2014**, *5*, 2027–2032.

(22) Bedrov, D.; Ayyagari, C.; Smith, G. D. Multiscale Modeling of Poly(ethylene oxide)-Poly(propylene oxide)-Poly(ethylene oxide) Triblock Copolymer Micelles in Aqueous Solution. *J. Chem. Theory Comput.* **2006**, *2*, 598–606.

(23) Al-Anber, Z. A.; Bonet Avalos, J.; Mackie, A. D. Prediction of the Critical Micelle Concentration in a Lattice Model for Amphiphiles Using a Single-Chain Mean-Field Theory. *J. Chem. Phys.* **2005**, *122*, 104910.

(24) Rosenbluth, M. N.; Rosenbluth, A. W. Monte Carlo Calculation of the Average Extension of Molecular Chains. *J. Chem. Phys.* **1955**, *23*, 356–359.

(25) De Nicola, A.; Kawakatsu, T.; Milano, G. A Hybrid Particle-Field Coarse-Grained Molecular Model for Pluronics Water Mixtures. *Macromol. Chem. Phys.* **2013**, *214*, 1940–1950.

(26) Nawaz, S.; Carbone, P. Coarse-Graining Poly(ethylene oxide)-Poly(propylene oxide)-Poly(ethylene oxide) (PEO-PPO-PEO) Block Copolymers Using the MARTINI Force Field. *J. Phys. Chem. B* **2014**, *118*, 1648–1659.

(27) Aharoni, S. M. On entanglements of flexible and rodlike polymers. *Macromolecules* **1983**, *16*, 1722–1728.

(28) Mortensen, K. Structural studies of aqueous solutions of PEO - PPO - PEO triblock copolymers, their micellar aggregates and mesophases; a small-angle neutron scattering study. *J. Phys.: Condens. Matter* **1996**, *8*, A103–A124.

(29) Malcolm, G. N.; Rowlinson, J. S. The thermodynamic properties of aqueous solutions of polyethylene glycol, polypropylene glycol and dioxane. *Trans. Faraday Soc.* **1957**, *53*, 921–931.

(30) Bailey, A.; Salem, B.; Walsh, D.; Zeytountsian, A. The interfacial tension of poly(ethylene oxide) and poly(propylene oxide) oligomers. *Colloid Polym. Sci.* **1979**, *257*, 948–952.

(31) Helfand, E.; Tagami, Y. Theory of the interface between immiscible polymers. *J. Polym. Sci., Part B: Polym. Lett.* **1971**, *9*, 741–746.

(32) Press, W. H.; Teukolsky, S. A.; Vetterling, W. T.; Flannery, B. P. *Numerical Recipes 3rd Edition: The Art of Scientific Computing*, 3rd ed.; Cambridge University Press: New York, NY, 2007; pp 515–520.

(33) Mortensen, K.; Pedersen, J. S. Structural study on the micelle formation of poly(ethylene oxide)-poly(propylene oxide)-poly(ethylene oxide) triblock copolymer in aqueous solution. *Macromolecules* **1993**, *26*, 805–812.

(34) Nolan, S. L.; Phillips, R. J.; Cotts, P. M.; Dungan, S. R. Light Scattering Study on the Effect of Polymer Composition on the Structural Properties of PEO-PPO-PEO Micelles. *J. Colloid Interface Sci.* **1997**, *191*, 291–302.

(35) Batrakova, E.; Lee, S.; Li, S.; Venne, A.; Alakhov, V.; Kabanov, A. Fundamental Relationships Between the Composition of Pluronic Block Copolymers and Their Hypersensitization Effect in MDR Cancer Cells. *Pharm. Res.* **1999**, *16*, 1373–1379.

(36) Yang, L.; Alexandridis, P.; Steytler, D. C.; Kositza, M. J.; Holzwarth, J. F. Small-Angle Neutron Scattering Investigation of the Temperature-Dependent Aggregation Behavior of the Block Copolymer Pluronic L64 in Aqueous Solution. *Langmuir* **2000**, *16*, 8555–8561.

(37) Wanka, G.; Hoffmann, H.; Ulbricht, W. Phase Diagrams and Aggregation Behavior of Poly(oxyethylene)-Poly(oxypropylene)-Poly(oxyethylene) Triblock Copolymers in Aqueous Solutions. *Macromolecules* **1994**, *27*, 4145–4159.

(38) Kabanov, A. V.; Nazarova, I. R.; Astafieva, I. V.; Batrakova, E. V.; Alakhov, V. Y.; Yaroslavov, A. A.; Kabanov, V. A. Micelle Formation and Solubilization of Fluorescent Probes in Poly(oxyethylene-b-oxypropylene-b-oxyethylene) Solutions. *Macromolecules* **1995**, *28*, 2303–2314.

(39) Liu, Y.; Chen, S.-H.; Huang, J. S. Small-Angle Neutron Scattering Analysis of the Structure and Interaction of Triblock Copolymer Micelles in Aqueous Solution. *Macromolecules* **1998**, *31*, 2236–2244.

(40) Alexandridis, P.; Hatton, T. A. Poly(ethylene oxide)-poly(propylene oxide)-poly(ethylene oxide) block copolymer surfactants in aqueous solutions and at interfaces: thermodynamics, structure, dynamics, and modeling. *Colloids Surf., A* **1995**, *96*, 1–46.

(41) Alexandridis, P.; Holzwarth, J. F.; Hatton, T. A. Micellization of Poly(ethylene oxide)-Poly(propylene oxide)-Poly(ethylene oxide) Triblock Copolymers in Aqueous Solutions: Thermodynamics of Copolymer Association. *Macromolecules* **1994**, *27*, 2414–2425.

(42) Kozlov, M. Y.; Melik-Nubarov, N. S.; Batrakova, E. V.; Kabanov, A. V. Relationship between Pluronic Block Copolymer Structure, Critical Micellization Concentration and Partitioning Coefficients of Low Molecular Mass Solutes. *Macromolecules* **2000**, *33*, 3305–3313.

(43) Goldmints, I.; von Gottberg, F. K.; Smith, K. A.; Hatton, T. A. Small-Angle Neutron Scattering Study of PEO-PPO-PEO Micelle Structure in the Unimer-to-Micelle Transition Region. *Langmuir* **1997**, *13*, 3659–3664.

(44) Wu, G.; Chu, B.; Schneider, D. K. SANS Study of the Micellar Structure of PEO/PPO/PEO Aqueous Solution. *J. Phys. Chem.* **1995**, *99*, 5094–5101.

(45) Almgren, M.; Bahadur, P.; Jansson, M.; Li, P.; Brown, W.; Bahadur, A. Static and dynamic properties of a (PEO-PPO-PEO) block copolymer in aqueous solution. *J. Colloid Interface Sci.* **1992**, *151*, 157–165.

(46) Mortensen, K.; Brown, W. Poly(ethylene oxide)-poly(propylene oxide)-poly(ethylene oxide) triblock copolymers in aqueous solution. The influence of relative block size. *Macromolecules* **1993**, *26*, 4128–4135.

(47) Booth, C.; Attwood, D. Effects of block architecture and composition on the association properties of poly(oxyalkylene) copolymers in aqueous solution. *Macromol. Rapid Commun.* **2000**, *21*, 501–527.

(48) Burczyk, B.; Wilk, K. A.; Sokołowski, A.; Syper, L. Synthesis and Surface Properties of N-Alkyl-N-methylgluconamides and N-Alkyl-N-methyllactobionamides. *J. Colloid Interface Sci.* **2001**, *240*, 552 – 558.

(49) Rosen, M. J.; Mathias, J. H.; Davenport, L. Aberrant Aggregation Behavior in Cationic Gemini Surfactants Investigated by Surface Tension, Interfacial Tension, and Fluorescence Methods. *Langmuir* **1999**, *15*, 7340–7346.

(50) Nikoubashman, A.; Panagiotopoulos, A. Z. Communication: Effect of solvophobic block length on critical micelle concentration in model surfactant systems. *J. Chem. Phys.* **2014**, *141*, 041101.

Graphical TOC Entry